CPM Specifications Document
Kawasaki Disease:

OSMSC 0108_0000

May 27, 2013

Version 1

Open Source Medical Software Corporation

1. Clinical Significance & Condition

Kawasaki disease is the leading cause for acquired pediatric heart disease in developed countries [1]. KD is diagnosed in over 5,500 patients annually in the U.S [2]. It is an acute vasculitis/inflammation of vessels [1]. KD is usually diagnosed in children under 5 years of age with an average age of 2 [2, 3]. The disease is almost twice as common in boys than in girls [3].

The cause for the disease is unknown, however the seasonality and acute nature of cases suggests an infectious trigger even though no causative agent has been identified. Furthermore, genetic susceptibility to the disease and outcomes of the disease has also been observed, particularly in Asian populations. Thus, it is generally proposed that KD results from exposure to a causative agent that triggers the disease in genetically predisposed hosts [1].

Presented symptoms in infancy and early childhood that lead to diagnosis include fever for at least 4 days, rashes, erythema of the lips and oropharynx, swollen tongue ("strawberry tongue"), edema of the hands and feet, and erythema of the palms and soles often followed by periungual desquamation [1]. Coronary aneurysms, the most serious complication related to KD may develop in up to 25% of patients with untreated KD and increase the risk of thrombosis, stenotic lesions, and myocardial infarction [2, 1]. Duration of fever has shown to correlate strongly with increased risk for coronary aneurysms. The most common sites for coronary aneurysms, in order of highest to lowest frequency are the: (1) proximal Left anterior descending artery (LAD) and right coronary artery (RCA), (2) left main coronary artery (LMCA), (3) left circumflex artery (LCX), (4) and lastly the junction between the RCA and right posterior descending artery (RPD) (Figure 1) [4].

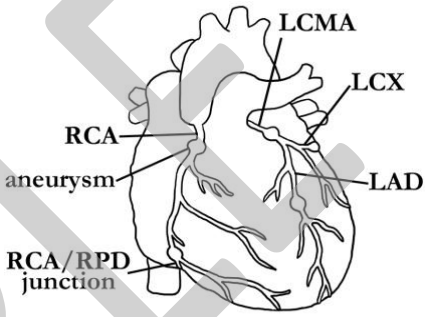

Figure 1: Common Sites of coronary aneurysms for KD patients

KD patients are usually treated with aspirin and intravenous immunoglobulin (IVIG) [1]. Aspirin serves to reduce acute symptoms while IVIG is thought to reduce the risk of developing coronary aneurysms from 25% to 3-5% if administered within 10 days after fever onset [1]. Conticosteriods, pentoxifylline, ulinastatin, abciximab and other drugs may also be used as treatment, and are sometimes used when IVIG treatments fail. Echoardiography is then used to evaluate cardiac state and assess appropriate longitudinal follow-up treatment. Children can usually return to normal activity after the acute episode subsides, however if cardiac anomalities are detected periodic clinical assessment after the acute episode is scheduled [5]. If an initially detected coronary aneurysm does not disappear properly or if an aneurysm develops in the long-term, the aneurysm often narrows in attempt to heal resulting in a stenosis or a blood clot in the aneurysm site may also cause obstruction. Obstructive lesions in Kawasaki patients are usually treated with a coronary artery bypass graft, where an artery or vein from the patient is used to bypass the obstruction and provide blood downstream of the obstruction (Figure 2). The use of stenting, rotational ablation, and balloon angioplasty has been limited in Kawasaki patients and are often unfavorable alternatives to coronary artery bypass [4].

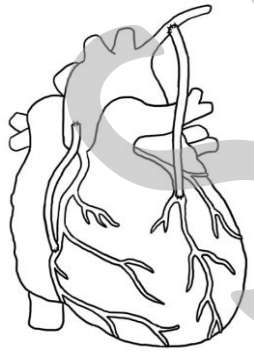

Figure 2: Coronary artery bypass graft

2. Clinical Data

Patient-specific volumetric image data was obtained to create physiological models and blood flow simulations. Details of the imaging data used can be seen in Table 1. See Appendix 1 for details on image data orientation.

Table 1 – Patient-specific volumetric image data details (mm). Voxel Spacing, voxel dimensions, and physical dimensions are provided in the Right-Left (R), Anterior-Posterior (A), and Superior-Inferior (S) direction.

OSMSC ID	Modality	Voxel Spacing			Voxel Dimensions			Physical Dimensions		
		R	A	S	R	A	S	R	A	S
0108_0000	CT	0.4492	0.4492	0.6250	512	512	273	230.00	230.00	170.63

Patient specific clinical data can be found in Table 2.

Table 2 – Available patient-specific clinical data

OSMSC ID	Age	Gender	BSA	Heart Rate	Stroke Volume (mL)	Cardiac Output (L/min)	Systolic Pressure (mmHg)	Diastolic Pressure (mmHg)
0108_0000	10	M	1.16	59	58	3.4	52	105

3. Anatomic Model Description

Anatomic models were created using customized SimVascular software (Simtk.org) and the image data described in Section 2. The model extends from the ascending aorta to the location in the descending aorta just above the celiac trunk. See

Table 3 for a visual summary of the image data, paths, segmentations and solid model constructed.

Table 3 – Visual summary of image data, paths, segmentations and solid model.

OSMSC ID	Image Data	Paths	Paths and Segmentations	Model
ID: OSMSC0108 subID: 0000 Age: 10 Gender: M	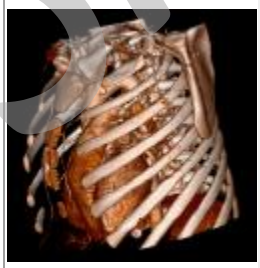	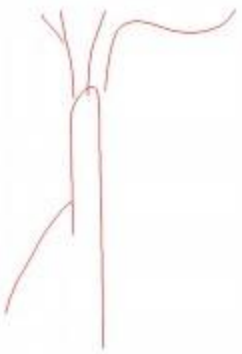	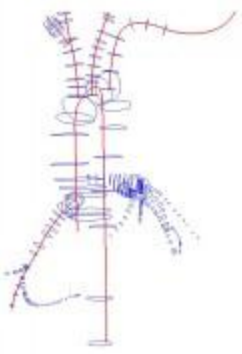	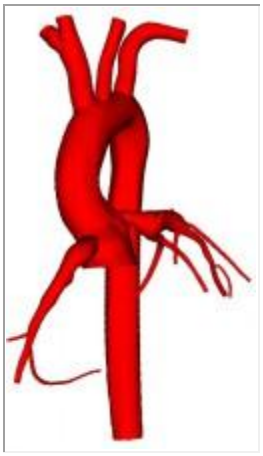

Details of anatomic models, such has number of outlets and model volume, can be seen in Table 4.

Table 4 – Anatomic Model details

OSMSC ID	Inlets	Outlets	Volume (cm^3)	Surface Area (cm^2)	Vessel Paths	2-D Segmentations
0108_0000	1	15	62.987	194.447	6	215

4. Physiological Model Description

In addition to the clinical data gathered for this model, several physiological assumptions were made in preparation for running the simulation. See Appendix 3 for details.

5. Simulation Parameters & Details

5. 1 Simulation Parameters

See Appendix 4 and the publication featuring this model [6] for information on the physiology and simulation specifications. Solver Parameters can be found in

Table 5- Solver Parameters

OSMSC ID	Time Steps Per Cardiac Cycle	Time Stepping Strategy
0108_0000	1000	fixed_step 3

5. 2 Inlet Boundary Conditions

A typical aortic waveform was prescribed to the inlet of the computational fluid dynamics (CFD) model (Figure 3). The waveform was scaled to be consistent with the cardiac output and heart rate calculated from clinical data. See Table 6 for the period and prescribed cardiac inflow for each simulation.

Table 6 – Period and Cardiac Output from waveforms seen in Figure 3

OSMSC ID	Period (s)	Cardiac Output (L/min)	Profile Type
0108_0000	1.017	3.4	Parabolic

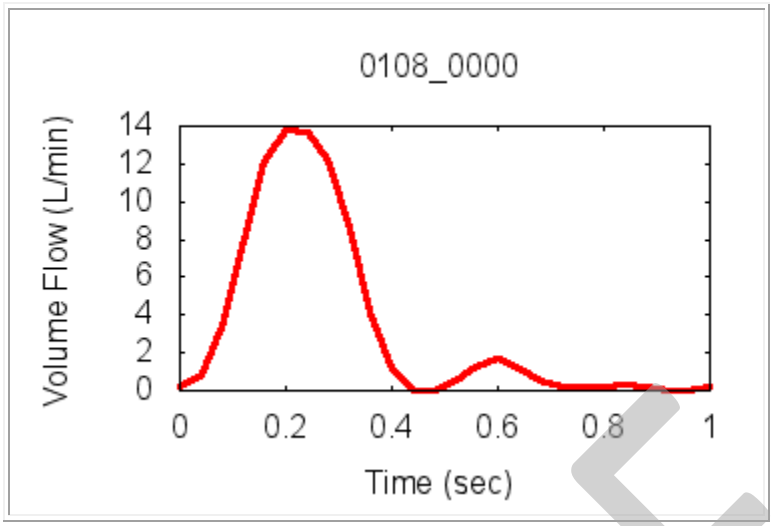

Figure 3 – Inflow waveforms in L/min

5. 3 Outlet Boundary Conditions

A three element Windkessel model was applied at the descending aorta, subclavian, and carotid outlets. For more information refer on RCR parameters to Exhibit 1 and Appendix 5. To define the parameters in the Windkessel model the mean flow to the aorta outlet was assumed to be 96% of the cardiac output. The coronary arteries were assumed to take 4% of the cardiac output with a split of 60% and 40% for the left and right coronary arteries respectively. Lumped parameter boundary conditions were applied at the coronary outlets using the coupled domain method [6]. Coronary boundary condition parameters were tuned to match target flow splits and pressures. Coronary Boundary parameters can be found in Exhibit 1. Target Pressures for both models were set based on clinically acquired data. See Table 6 for target flow splits and pressures.

Table 7 – Flow distributions and Pressures

OSMSC ID	Coronary Flow	Left Coronary Flow	Right Coronary Flow	Disastolic Pressure (mmHg)	Systolic Pressure (mmHg)
0108_0000	4%	60%	40%	52	105

6. Simulation Results

Simulation results were quantified for the last cardiac cycle. Paraview (Kitware, Clifton Park, NY), an open-source scientific visualization application, was used to visualize the results. A volume rendering of velocity magnitude for three time points during the cardiac cycle can be seen in

Table 8 for the simulation.

Table 8 – Volume rendering velocity during peak systole, end systole, and end diastole.
All renderings have the scale below with units of cm/s

OSMSC ID	Peak Systole	End Systole	End Diastole
ID: OSMSC0108 subID: 0000 Age: 10 Gender: M	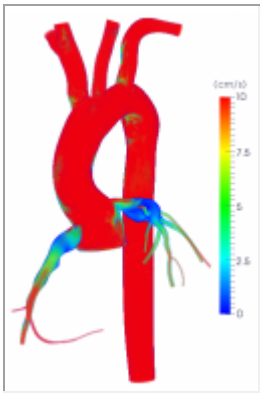	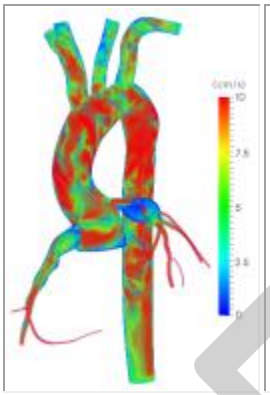	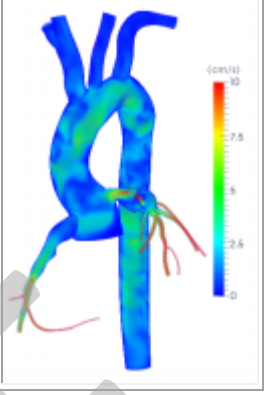

Surface distribution of time-averaged blood pressure (TABP), time-averaged wall shear stress (TAWSS) and oscillatory shear index (OSI) were also visualized and can be seen in Table 9.

Table 9 – Time averaged blood pressure (TABP), time-average wall shear stress (TAWSS), and oscillatory shear index (OSI) surface distributions

OSMSC ID	TABP	TAWSS	OSI
ID: OSMSC0108 subID: 0000 Age: 10 Gender: M	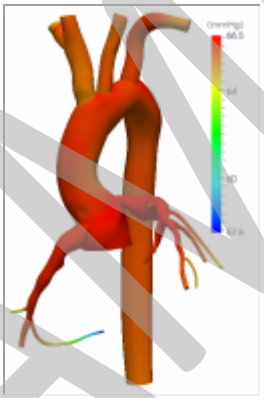	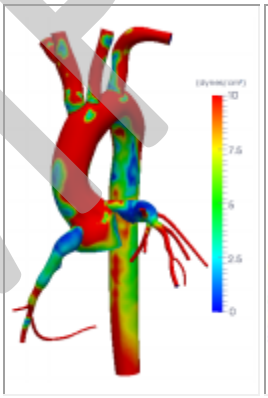	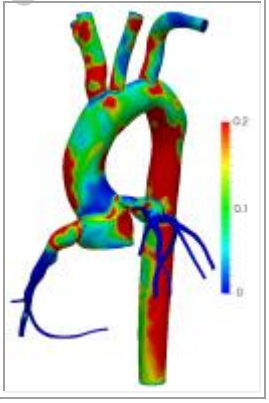

7. References

[1] J. B. Gordon, "When children with Kawasaki Disease grow up: myocardial and vascular complications in adulthood," *Journal of the American College of Cardiology,* vol. 54, no. 21, pp. 1911-1920, 2009.

[2] D. Sengupta, "Image-based modeling of hemodynamics in coronary artery aneurysms caused by Kawasaki disease," *Biomechanicd and Modeling in Mehcanobiology,* 2011.

[3] American Heart Association, "Kawasaki Disease," 6 October 2010. [Online]. Available: http://www.heart.org/HEARTORG/Conditions/More/CardiovascularConditionsofChildhood/Kawasaki-

Disease_UCM_308777_Article.jsp#.TyltYVx8AsI. [Accessed 1 January 2012].

[4] J. W. Newburger, "Diagnosis, Treatment, and Long-Term Management of Kawasaki Disease: A Statement for Health Professionals From the Committee on Rheumatic Fever, Endocarditis and Kawasaki Disease, Council on Cardiovascular Disease in the Young, American Heart Association," *Circulaton,* vol. 110, pp. 2747-2771, 2004.

[5] American Heart Association, "Kawasaki Disease: Complications, Treatment and Prevention," 25 August 2010. [Online]. Available: http://www.heart.org/HEARTORG/Conditions/More/CardiovascularConditionsofChildhood/Kawasaki-Disease-Complications-Treatment-and-Prevention_UCM_311584_Article.jsp#.Tylu71x8AsI. [Accessed 1 February 2012].

[6] D. Segupta, A. M. Kahn, J. C. Burns, S. Sankaran, S. C. Shadden and A. L. Marsden, "Image-based modeling of hemodynamics in coronary srtery aneurysms caused by Kawasaki disease," *Biomechanicacs and Modeling in Mechanobiology,* 2011.

[7] D. Sengupta, A. M. Kahn, J. C. Burns, S. Sankaran, S. C. Shadden and A. L. Marsden, "Image-based modeling of hemodynamics in coronary srtery aneurysms caused by Kawasaki disease," *Biomechanicacs and Modeling in Mechanobiology,* 2011.

Exhibit 1: Coronary Simulations Boundary Conditions

Information on how RCR values were obtained is included in Appendix 5. RCR values for the final simulation are shown on Table 10. Coronary boundary parameters and Intramyocardial pressure plots from Sungupta et. al (2011) for each simulation are shown on Table 11 and, respectively [2].

Table 10 – RCR Values for 0108_0000

OSMSC ID	Solver ID	Face Name	Artery Name	Rp	C	Rd
0108_0000	3	aorta_br1	Right Subclavian	1925.72	0.000245	10418.66
0108_0000	4	aorta_br2	Right Common Carotid	1896.88	0.000249	10262.58
0108_0000	5	aorta_br3	Left Common Carotid	2438.49	0.000193	13192.83
0108_0000	6	aorta_br4	Left Subclavian	2681.73	0.000176	14508.84
0108_0000	2	aorta_outlet	Descending Aorta	553.79	0.000852	2996.129

Table 11- Coronary Boundary Parameters for 0108_0000

OSMSC ID	Solver ID	Face Name	dQinidT	dPinidT	q0	q1	q2	p0	p1	p2	b0	b1	b2
0108_0000	7	outlet_lc_br1	0	100	414875.3	284692.9	7902.9	1	0.89941	0.06100	0	0.79592	0
0108_0000	8	outlet_lc_br2	0	100	1060255.1	727560.9	20196.6	1	0.89941	0.06100	0	0.79592	0
0108_0000	9	outlet_lc_br3	0	100	265523.5	182205.7	5057.9	1	0.89941	0.06100	0	0.79592	0
0108_0000	10	outlet_lc_br4	0	100	414875.3	284692.9	7902.9	1	0.89941	0.06100	0	0.79592	0
0108_0000	11	outlet_lc_br5	0	100	327843.7	224970.6	6245.0	1	0.89941	0.06100	0	0.79592	0
0108_0000	12	outlet_lc_br6	0	100	737555.8	506120.4	14049.6	1	0.89941	0.06100	0	0.79592	0
0108_0000	13	outlet_lc_main	0	100	265523.5	182205.7	5057.9	1	0.89941	0.06100	0	0.79592	0
0108_0000	14	outlet_rc_br1	0	100	271483.2	36366.3	382.1	1	0.18524	0.00445	0	0.14485	0
0108_0000	15	outlet_rc_br2	0	100	306271.4	41026.4	431.0	1	0.18524	0.00445	0	0.14485	0
0108_0000	16	outlet_rc_main	0	100	212691.0	28490.9	299.3	1	0.18524	0.00445	0	0.14485	0

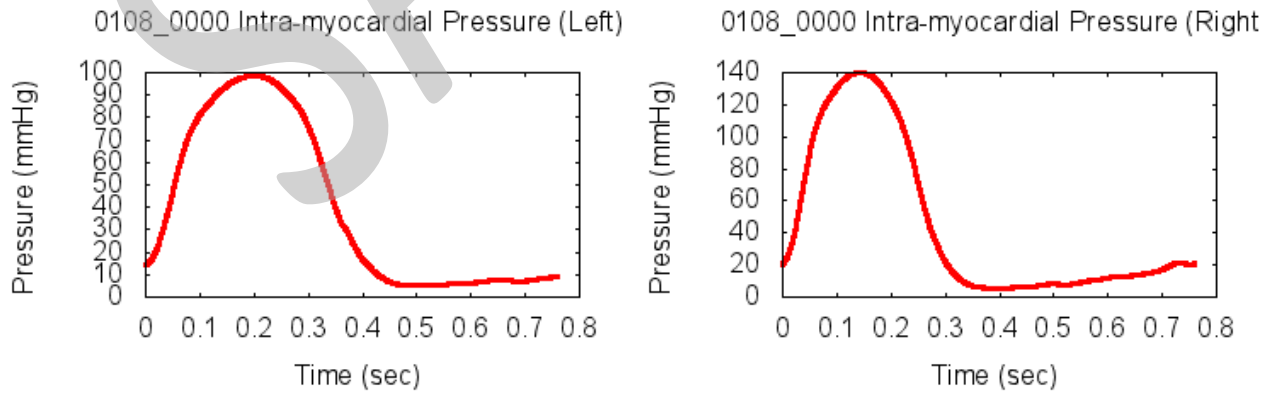

Figure 4- Left and Right Intramyocardial Pressure

Appendix

1. Image Data Orientation

The RAS coordinate system was assumed for the image data orientation. Voxel Spacing, voxel dimensions, and physical dimensions are provided in the Right-Left (R), Anterior-Posterior (A), and Superior-Inferior (S) direction in all specification documents unless otherwise specified.

2. Model Construction

All anatomic models were constructed in RAS Space. The models are generated by selecting centerline paths along the vessels, creating 2D segmentations along each of these paths, and then lofting the segmentations together to create a solid model. A separate solid model was created for each vessel and Boolean addition was used to generate a single model representing the complete anatomic model. The vessel junctions were then blended to create a smoothed model.

3. Physiological Assumptions

Newtonian fluid behavior is assumed with standard physiological properties. Blood viscosity and density are given below in units used to input directly into the solver.

Blood Viscosity: 0.04 g/cm•s^2
Blood Density: 1.06 g/cm^3

4. Simulation Parameters

Conservation of mass and Navier-Stokes equations were solved using 3D finite element methods assuming rigid and non-slip walls. All simulations were ran in cgs units and ran for several cardiac cycles to allow the flow rate and pressure fields to stabilize.

5. Outlet Boundary Conditions

5.1 Resistance Methods

Resistances values can be applied to the outlets to direct flow and pressure gradients. Total resistance for the model is calculated using relationships of the flow and pressure of the model. Total resistance is than distributed amongst the outlets using an inverse relationship of outlet area and the assumption that the outlets act in parallel.

5.2 Windkessel Model

In order to represent the effects of vessels distal to the CFD model, a three-element Windkessel model can be applied at each outlet. This model consists of proximal resistance (R_p), capacitance (C), and distal resistance (R_d) representing the resistance of the proximal vessels, the capacitance of the proximal vessels, and the resistance of the distal vessels downstream of each outlet, respectively (Figure 1).

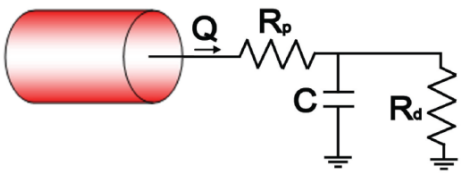

Figure 5 - Windkessel model

First, total arterial capacitance (TAC) was calculated using inflow and blood pressure. The TAC was then distributed among the outlets based on the blood flow distributions. Next, total resistance (R_t) was calculated for each outlet using mean blood pressure and PC-MRI or calculated target flow ($R_t=P_{mean}/Q_{desired}$). Given that $R_t=R_p+R_d$, total resistance was distributed between R_p and R_d adjusting the R_p to R_t ratio for each outlet.